Advanced Pharmaceutical Bulletin

Accepted Manuscript (unedited)

The manuscript will undergo copyediting, typesetting, and review of the resulting proof before it is published in its final form.

Research Article

How to cite this article:
Teiama MS, Sakran W, Masry F, Abdel Gaber S, Ali R. Study the Synergistic Effect of Combination Therapy Containing Temozolomide and N-Acetylcysteine Loaded Polymeric Micelles in Cancer Treatment. Advanced Pharmaceutical Bulletin, doi: 10.34172/apb.47566

Study the Synergistic Effect of Combination Therapy Containing Temozolomide and N-Acetylcysteine Loaded Polymeric Micelles in Cancer Treatment

Mohammed Salah. Teiama [*a, b], Wedad Elsayed Sakran [a], Fares Ibrahim Masry [a], Sara Ahmed. Abdel Gaber [c], and Raghda abd el moneum Ali[a]

[a] Department of Pharmaceutics and Industrial Pharmacy, Faculty of Pharmacy, Capital University (Formal Helwan University), Ain Helwan, POB 11795, Cairo, Egypt
[b] Department of Pharmaceutics and Industrial Pharmacy, Faculty of Pharmacy, Galala University, Attaka 43713, Suez, Egypt
[c] Clinical Pharmacy Department, Faculty of Pharmacy, Egypt-Japan University of Science and Technlogy, New Borg El-Arab, Alexandria, Egypt

ARTICLE INFO

Keywords:
Glioblastoma,
N-acetylcysteine,
Polymeric micelle,
Synergism,
Temozolomide

Article History:
Submitted: June 15, 2026
Revised: August 08, 2026
Accepted: August 14, 2026
ePublished: September 05, 2026

ABSTRACT

Purpose: The aim of this study was to develop TMZ-NAC loaded polymeric micelles (TNPM), evaluate them in vitro, and study the synergistic effect between Temozolomide (TMZ) and N-acetylcysteine (NAC) on the human glioblastoma multiforme A172 cell line (HGM-A172).
Methods: Six (TNPM) formulations (F1 to F6) were fabricated by pluronic p-123 (P123) and pluronic p-188 (P188) at different molar percentages using a modified thin-film hydration method. The formula F5 provided the highest percentage of drug loading for TMZ and NAC. Thus, different ratios of the two drugs were loaded in polymeric micelles (PM) with molar percentage (80:20) of P123:P188 to form eight TNPM formulations (L1 to L8) that were evaluated for cytotoxic effect against (HGM-A172).
Results: TNPM formulations (L2, L3 and L4) provided the lowest IC_{50} (31.5±0.38 µg/ml, 19.94±0.15 µg/ml and 18.3±0.21 µg/ml, respectively). Furthermore, Characterization of the selected (L2 and L4) was done. Moreover, the formula (L4) was selected according to the previous characterization for in vitro release studies, cell cycle analysis, cell apoptosis and cellular uptake. The L4 showed an average particle size 25.39±10.31 nm and zeta potential -24.5±4.8 mV. The DSC and FT-IR analysis confirmed the encapsulation of both drugs within PM. TNPM (L4) provided a 1.783-fold increase in the dissolution efficiency (%) of TMZ, compared to pure TMZ. The cellular uptake efficiency after 24 h was 30.48 and 15 folds higher than the free TMZ and free NAC, respectively.
Conclusion: The combination index calculation, cell cycle analysis and cell apoptosis confirmed the cytotoxic synergistic effect between TMZ and NAC in L4 against (HGM-A172).

***Crossponding Author**
Mohammed Salah Ahmed Teiama, Email: dr_mteiama84@pharm.helwan.edu.eg, ORCID: 0000-0002-3980-4036

Introduction

Loading multiple drugs with different mechanisms onto the same drug-delivery nanocarrier in a precisely controllable manner is an innovative approach and a promising tool to improve the efficacy of the drug low doses against the cancer resistance and maximize the synergistic output of drug combination. This delineation is crucial to defeating the side effects of drugs in the treatment of central nervous system diseases and tumors.[1] During the past years, the incidence and death rate from brain tumors increased several-fold in all countries, until brain tumors became one of the most fatal cancers causing death worldwide. This is reflected in its ranking as the 17th most common cancer and accounts for 1-2% of all tumors.[2] In this category, the most prevalent type of primary brain cancer is malignant glioma that usually initiates from the glial cells.[3] Malignant gliomas includes different types of tumor such as glioblastoma multiforme (GBM) which represents the most aggressive and lethal brain tumor with a higher incidence rate in males than in females (1.6 times) at a median age of 64 years old. [4] Despite the treatment approach, GBM exhibits a poor survival rate that does not exceed one year in most cases. [5]

Temozolomide (TMZ) is a typical chemotherapeutic agent for treatment of GBM. Its mechanism in cancer cell death arises by its methylation which induces DNA degradation, therefore TMZ is classified as an alkylating agent. However, TMZ has poor bioavailability and therapeutic efficacy in the brain due to poor permeability through the tumor cell membrane and the blood-brain barrier (BBB) .[6] Although TMZ is the most typical and efficient chemotherapeutic agent for treatment of GBM, the primary tumor exhibits a recurrence as a result of the drug resistance.[7] TMZ has high oral bioavailability (almost 100%) [8], due to the adequate solubility, particularly in the acidic conditions of the stomach [9] and a relatively short half-life of about 1.8 h.[10] It is a prodrug that converts to an active metabolite, MTIC, which is responsible for its cytotoxic effects.[11] The drug is rapidly absorbed from the gastrointestinal tract by passive diffusion [10], reaching peak plasma concentrations within an hour.[8] TMZ is primarily eliminated through renal excretion [10], with minimal liver metabolism.[12] Unfortunately, TMZ has rapid elimination rate, short shelf life, and poor bioavailability in brain (20%) which required frequent doses and causes several side effects.[13]

N-Acetylcysteine (NAC) is a typical mucolytic agent with antioxidant activity and is used in the treatment of acetaminophen poisoning.[14] NAC is widely used for the treatment of several neurodegenerative disorders such as mild to moderate brain trauma and injury. Moreover, it could be used for the treatment of neuropsychiatric disorders such as Parkinson's and Alzheimer's disease, schizophrenia, depression, and bipolar disorder as well as smoking, cannabis, and cocaine addictions.[15] Recent data shows that NAC improves the cancer treatment process by its chemo-preventive action.[16] However, high doses of NAC exhibit undesirable side effects such as; emesis, diarrhea, and headache.[4,17,18] Additionally, significant cytotoxicity in dopaminergic neurons was reported with the administration of NAC high doses as a result of glutathione overproduction.[17] Thus, modifying the requirement of NAC high doses is a great necessity via fabrication of a delivery system with high access and permeability to the brain. Recently, the administration of two or more anticancer drugs with different mechanisms on the same carrier was studied as an outstanding approach to improve the pharmacological activities of drugs and defeat the drug resistance even at low drug doses. This strategy could be helpful in the treatment of CNS diseases to reduce possible side effects. Among the many available adjuvant molecules, we highlight the co-administration of TMZ with NAC as a dual therapy.

Recently, nanoparticles have been utilized as a promising carrier for the co-administration of multiple drugs offering several advantages.[18] The individual administration of the free drugs will exhibit variant pharmacokinetic parameters with poor allocation and distribution of the drugs at the tumor site accompanied with severe systemic damage. The loading of two or more drugs into a single nanocarrier might be the way to show precise and

controlled release of the drugs in balanced ratios, which can improve the chemical stability, biodistribution, and pharmacokinetics of dissimilar drugs that independently have disparate therapeutic behaviors [19]

Among various nanocarriers, micelles attract great attention owing to their unique core shell construction which provide an adjustable loading zone for hydrophobic drug as well as a hydrophilic one; diminishing the self-aggregation, clearance by nonspecific uptake by the reticuloendothelial system (RES), and plasma proteins binding.[20,21] Moreover, they consist of two main units; lipophobic poly (ethylene oxide) (PEO) and lipophilic poly (propylene oxide) which arranged in a PEO–PPO–PEO triblock. This arrangement increases the circulation of pluronics in the blood for a longer time which sustained the drug therapeutic activity and diminish the side effect of chemotherapeutic agent.[20] As mentioned before, pluronic copolymers are inert carriers that can minimize the multi-drug-resistant mechanism (MDR) to chemotherapeutic agents *in vitro* and *in vivo* through inhibition of P-glycoprotein.[22] The size of pluronic micelles provides another substantial feature which makes them more efficient and effective carriers for drugs.[23] The nano-size of pluronic micelles, combined with their long circulatory character, allows them to exploit the leaky vasculature of compromised tissues (the EPR phenomenon) and accumulate inside the tumor. Nano-micelles cannot escape from the interstitial spaces after internalization via EPR permeation. In contrast, smaller moieties can move into and out of the tumor via a diffusion mechanism.[24] Recently, some applications of chemotherapy-loaded pluronic micelles became available for patients, such as Genexol®-PM which consists of paclitaxel loaded with polymeric micelles.[25]

The objective of our work was to fabricate TMZ-NAC-loaded polymeric micelles (TNPM) and to evaluate their physicochemical properties, in vitro cytotoxicity, cell cycle, cell apoptosis, and cellular uptake, aiming to study the synergistic effect between TMZ and NAC on the human glioblastoma multiforme A172 cell line.

Experimental

Materials

Temozolomide (TMZ), Pluronic p-123® (P123) (Molecular weight: 5700 g/mol) and Pluronic p-188® (P188) (Molecular weight: 9510 g/mol) were bought from Sigma Aldrich (St. Louis, USA). N-acetylcysteine (NAC) was gifted by SEDICO pharmaceutical company, Egypt. Ethanol (LC-MS grade), hydrochloride acid, acetic acid and methanol were bought from Sigma Aldrich (Chemie GmbH, Steinheim, Germany). The human glioblastoma multiforme A172 cell line was purchased from the American Type Culture Collection (ATCC). Ultra-pure grade water used throughout the work was obtained from deionized water, PURELAB Prima, VWS Ltd. (ELGA- Lab Water Global Operation Centre, High Wycombe, HP14 3BY, Bucks, UK). All other chemicals and solvents that were utilized in our work, were commercially bought as analytical-grade materials.

1. Methodology

1.1 Fabrication of TMZ-NAC-loaded polymeric micelles

TMZ-NAC-loaded pluronic micelles were prepared simply via some modulation to the common thin-film hydration technique .[26] Briefly, P123 and P188 were dissolved in ethanol (4% w/v) along with a combination of TMZ and NAC at known ratios and then kept up to 1 min in water bath ultrasonicator (Table1). The thin film was obtained by evaporating the ethanol using a rotary evaporator (IKA, RV10B S99, HBIO basic, Deutschland, Germany) at 80 ℃ and 200 rpm, under constant known vacuum. Moreover, the film was dried completely of residual ethanol by storing it overnight at room temperature. Then, the obtained film was dispersed for 1-2 min at 80℃ with 10 mL of warmed distilled water, and finally sonicated for a further 1 min to obtain homogenous dispersion. In order to remove unencapsulated TMZ, the obtained TMZ-NAC-loaded micellar dispersion was filtered through micro-syringe filter with cellulose acetate membrane. While, unassociated NAC was removed by

a dynamic dialysis method with 100 ml of deionized water for 30 min for numerous times using a specific dialysis tube (MWCO: 12000–14000 Da, Livingstone, New South Wales, Australia).[27] When the drug could not be detected in the solution by a UV spectrophotometer at λ_{max} 214 nm, the dialysis process was terminated. The remaining dialyzed dispersion including TMZ-NAC loaded micelles were collected and lyophilized according to the following protocol. The prepared dispersions were collected in glass tubes and frozen at -70 °C for 24 h in an ultra-cold deep freezer. Subsequently, the samples were lyophilized using a lyophilizer Christ Alpha 1-2 LD (Osterode am Harz, Germany) for 24 h.[28] The lyophilized powder of TMZ-NAC-loaded micelle formulations were stored in desiccator for further investigations.

Table 1: Composition of prepared TMZ-NAC loaded micelle formulations

Formula No	Percent of pluronic		Ratio of two drugs	
	P 123	P 188	TMZ	NAC
F 1	20%	80%	1	1
F2	40%	60%	1	1
F3	50%	50%	1	1
F4	60%	40%	1	1
F5	80%	20%	1	1
F6	90%	10%	1	1

1.2. Determination of drug loading (DL) and entrapment efficiency (%EE)

The freeze dried TNPM formulations were weighed with an accurate digital balance and dissolved in known volume of 0.1N HCL and examined for both drugs using UV Spectrophotometer (Jasco, Japan). The %EE as well as the percent drug loading were calculated for both drugs in each preparation using the following equation:[29]

$$\%EE = \frac{\text{Actual drug content in (TNPM) formulation}}{\text{Total amount of drug fed initially}} \times 100 \qquad \text{Eq. (1)}$$

$$\%\ \text{Drug loading} = \frac{\text{Actual drug content in (TNPM) formulation}}{\text{wt of (TNPM) formulation}} \times 100 \qquad \text{Eq. (2)}$$

According to the obtained CMC *(the Supplementary Data Section S1.2)*, TNPM (L1 to L8) was fabricated as mentioned before using 80% P123 and 20% P188 with different ratios of both drugs (Table 2).

Table 2: Composition of prepared TNPM formulations with (80% P123 and 20%P188)

Formula	Ratios of two drugs		Pluronic ratio	
	TMZ	NAC	P 188	P 123
L1	1 (6.6mg)	2 (13.3mg)	20	80
L2	1 (5mg)	3 (15mg)	20	80
L3	1 (4mg)	4 (16mg)	20	80
L4	1 (3.33mg)	5 (16.6mg)	20	80
L5	5 (16.6mg)	1 (3.33mg)	20	80
L6	4 (16mg)	1 (4mg)	20	80
L7	0.00	(5mg)	20	80
L8	(15mg)	0.00	20	80

1.3. *In vitro* characterizations of developed TNPM formulations

1.3.1. Determination of drug loading (%DL) and entrapment efficiency (%EE)

The entrapped amounts of both drugs were evaluated as %DL as well as %EE for all the developed TNPM formulations as mentioned before in section (1.2)

1.3.2. Cytotoxicity determination

Cell culture procedures are provided in the Supplementary Data (Section S1.3).

1.3.2.1. Assessment of glioblastoma multiform cell viability in response to treatment

Cells were seeded in cell-culture treated flat bottom 96 well plates at cell density of $1x10^5$ cells/well and cultured till reaching a confluence level of 80%. Cells were then incubated with the preparations for 48 hrs. Eight solutions of known concentration were prepared from the eight formulations (L1-L8); each solution contained a known weight of the formula (1 mg/ml), with each formula containing TMZ and NAC according to its % drug loading. Solutions of known concentration were also prepared from pure TMZ (1 mg/ml), pure NAC (1 mg/ml), and the pure (blank) formula (1 mg/ml). One group of cells was incubated with only the complete medium and utilized as control group (reference group). Thus, the viable cell count was measured by applying MTT technique as described earlier.[30] The cell viability percentage was calculated as a ratio relative to the control group. The IC50 values (the concentration required to kill 50% of the cell population) were determined with a 95% confidence interval.[31]

1.3.3. Calculation of combination Index Values

The therapeutic effect of the combination between TMZ and NAC was estimated using the combination index (CI) technique established by **Chou and Talalay 2010**. The combination index value could be estimated via determination of the IC_{50} values for individual drugs and in combination as described previously.[32] The following equation is mainly used to calculate the CI values:

$$CI = \frac{D_{c1}}{D_{s1}} + \frac{D_{c2}}{D_{s2}} + \frac{D_{c1}D_{c2}}{D_{s1}D_{s2}}$$ **Eq (3)**

where *D*s1 and *D*s2 represent the IC_{50} of individual application of TMZ and NAC, while the IC_{50} values of TMZ and NA in combination are represented by *D*c1 and *D*c2, respectively. The outcome of the TMZ and NAC combination could be explained according to the obtained CI value as following: CI < 0.9, synergism; = 0.9 – 1.1, additive effect; > 1.1, antagonism.[32]

1.4. Characterization of the selected TNPM (L2 and L4)

The TMZ-NAC loaded formulations L2 & L4 were selected according to IC_{50} value for further characterization, investigation and obtained results. The morphology of L2 and L4 were screened using transmission electron microscopy (TEM). Furthermore, Fourier transform infra-red (FT-IR), differential scanning calorimetry (DSC), particle size, and zeta potential were carried out. Furthermore, the most optimized formula according to the obtained results was investigated using *in vitro* release studies, cell cycle analysis, *in vitro* cell apoptosis and cellular uptake [33].. Detailed protocols for TEM, DSC, and FT-IR characterization are provided in the Supplementary Data (Sections S1.4-S1.6).

1.4.1. Determination of particle size, zeta potential, and polydispersity index (PDI).

The mean particle size, surface charge (ZP), and polydispersity index (PDI) of the chosen formulations (L2 and L4) were examined using Malvern® Zetasizer (Worcestershire, UK). The chosen samples (L2 & L4) were diluted suitably with distilled water prior to measurements. The measurement was carried out at 25 ± 0.5 ℃ in triplicates and results were reported as mean value ± standard deviation (SD).

1.5. *In-vitro* release studies

The experimental work was carried out for the selected TNPM (L4) formula and the pure drugs (TMZ & NAC) using a dialysis bag technique in acetate-buffered saline (pH = 4.5) solution as the release medium in the presence of 0.1% Tween 80.[33] Acetate buffer (pH 4.5) was selected as the release medium not only to simulate the tumor microenvironment but also to ensure the chemical stability of TMZ throughout the 30 h testing period, as TMZ is highly stable against degradation under acidic conditions (pH < 5). Sample handling times were strictly controlled, and samples were stored under refrigerated conditions prior to immediate spectrophotometric assay. The dialysis membrane (MWCO: 12–14 kDa, Livingstone, New South Wales, Australia) was immersed overnight in the release medium. Amounts of TMZ-NAC-loaded PM (L4) equivalent to 25 mg of TMZ and 50.6 mg of NAC, as well as 25 mg of pure TMZ and 50.6 mg of pure NAC, were introduced into the dialysis membrane, which was tied at both ends to form a dialysis bag. Samples were soaked into 40 ml of release medium at 37°C ± 0.5°C and stirred with a small magnetic stirring bar at 100 rpm of stirring rate .[34] At certain time intervals of 0.25, 0.5, 1, 2, 4, 6, 8, 12, 16, 24 and 30 h, 1 ml was withdrawn from the release medium and immediately replaced with fresh medium. The withdrawn samples were filtered through a membrane syringe filter and examined spectrophotometrically for TMZ and NAC content at λ_{max} 324nm and 214nm, respectively. The experiment was carried out in triplicate and the mean values were represented as a graphical plot for the cumulative percent drug released ± standard deviation on Y-axis against time intervals on X-axis.

Furthermore, the release profile of TNPM (L4) was compared with the release profiles of both pure drugs using the dissolution efficiency (%DE), difference factor (f_1), and similarity factor (f_2). Difference factor (f_1) and similarity factor (f_2) were calculated using the known reported equations: [35]

$$f_1 = \left[\frac{[\sum_{t=1}^{n}|R_t - T_t|]}{\sum_{t=1}^{n} R_t}\right] \times 100 \qquad \textbf{Eq.(4)}$$

$$f_2 = 50.log\left\{\left[1 + \frac{1}{n}\sum_{t=1}^{n}(R_t - T_t)^2\right]^{-0.5}.100\right\} \qquad \textbf{Eq.(5)}$$

Where, the f_1 is utilized to detect the relative error between the release profiles of different samples by calculating the percent difference between the two curves of the examined samples at each time point. While, n represents the number of time points that were selected for the comparison. R_t represents the dissolution value of the reference (pure drug) at time t, and T_t is termed as the dissolution value of the test at time t. The two profiles are considered dissimilar when the f_1 value exceeds 15.0 or the f_2 value falls below 50.$f_1 f_2$

Moreover, the dissolution efficiency (%DE) was calculated according to the following equation**.** [36]

$$DE\ \% = \frac{\int_0^t y \times dt}{y_{100} \times t} \times 100\% \qquad \textbf{Eq. (6)}$$

Where y represents the percent of drug dissolved at time t and the areas under the curves were calculated using the trapezoidal method. The dissolution efficiency (%DE) was calculated until 30 h.

1.6. Release kinetics and mechanisms

The results of *in vitro* release studies were analyzed for the fitting to various kinetics models (zero order, first order and Higuchi) [37] as follows:

Zero order rate equation: $Q_t = Q_0 + k_0 t$ **Eq. (7)**

where Q_0 is initial amount of drug, Q_t is the amount of drug released at time *t*, K_0 is zero order release rate constant, *t* is time of sample determination.

First order rate equation: $\log Q = logQ_0 - \frac{k_1 t}{2.303}$ **Eq. (8)**

where Q_0 is the initial amount of drug, Q is the remaining amount of drug at time t, K_1 is first order release rate constant, and *t* is time of sample determination.

Higuchi's model: $Q = K_H\ t^{1/2}$ **Eq. (9)**

where *Q* is the amount of drug released in time *t* per unit area at time *t* , K_H is Higuchi diffusion rate constant.

The correlation coefficient (R^2) value was calculated to determine the best-fitted model.

To find out the mechanism of drug release from PM, the results of *in vitro* release study of (L4) were fitted to Korsmeyer and Peppas equation **:**[38] $\frac{M_t}{M_\infty} = kt^n$ **Eq. (10)**

Where, M_t / M_∞ is a fraction of drug release at time *t*, *K* is the release rate constant, and *n* is the release exponent. The value of exponent (*n*) is mainly utilized to indicate the mechanism of drugs release.

The n value, used to clarify the drug release pattern from TMZ-NAC-loaded PM (L4), was determined by plotting the log cumulative percentage of drug release (Y-axis) against log time (X-axis). Thus, the values of $n \leq 0.45$ indicate that drug release followed predominantly the controlled diffusion pattern (Fickian process). However, if the values of $n \geq 0.89$, the release pattern follows non-Fickian or case II transport type. When n ranges from 0.45 to 0.89, drug release follows an anomalous (non-Fickian) pattern, meaning it is controlled by a combination of diffusion and polymer relaxation. [38]

1.7. Cell cycle analysis using propidium iodide

A172 cells were treated with the determined IC50 of pure NAC, pure TMZ and L4 for 48 h in addition to a control group incubated only with complete medium. Then, the cells were trypsinized to be detached from the plates and the cell pellets were collected by centrifugation for 5 min at 251x g. Furthermore, the obtained pellets were washed by pre-warmed 1X PBS and fixed using 66% ethanol for 2 h at 4°C to be investigated using the cell

cycle arrest technique. Therefore, the cells were stained with Propidium Iodide (40 µL) and Ribonuclease A (50 µL) for 30 min. Stained cells were analyzed using flow cytometer (Excitation maximum = 493nm; Emission maximum = 636nm) and data were analyzed as described earlier.[39]

1.8. Evaluation of glioblastoma cell death mode in response to treatment

Human glioblastoma multiforme A172 cells were treated with the determined IC_{50} concentrations of pure NAC, pure TMZ and L4 for 48 h. A control group was included for comparison. Cells were trypsinised and the collected cell pellets were washed in 500 µL of 1X Binding Buffer prior to co-staining with Annexin V-FITC and Propidium Iodide according to the manufacturer´s protocol (BioVision Annexin V-FITC Apoptosis Detection Kit). Cells were tested by flow cytometry (Ex = 488 nm; Em = 530 nm) using FITC signal detector (FL1) and PI staining by the phycoerythrin emission signal detector (FL2) (Excitation maximum= 493 nm, Emission maximum = 636 nm). Obtained data were analyzed as described earlier.[39]

1.9. Cellular uptake studies

A172 cells were incubated with IC_{50} of free TMZ, free NAC and drugs loaded micelles (L4) for either 12 or 24 hrs. Untreated cells were kept with free medium and utilized as a control group. Afterward, the treated cells were washed three times with cold PBS.[40] The cells were trypsinized using a 0.25% trypsin solution (Gibco BRL, Carlsbad, USA) and were centrifuged to be concentrated in a pellet for further dilution. Pellets were homogenized in acetonitrile H_2O (50:50, v/v), sonicated in an ultrasonicator for 30 mins and centrifuged at 1000g for 10 min. The supernatants were collected and filtered through a 0.45 µm membrane prior the HPLC analysis for TMZ and NAC.[41]

TMZ and NAC in the collected samples were quantified by HPLC as detailed in the Supplementary Data (Section S1.8).

2. Results and discussion

2.1. Fabrication of TMZ-NAC-loaded polymeric micelle

As the micellar system of a single surfactant poloxamer exhibited many drawbacks; poor stability, low drug entrapment, and non-preferred large particle size, which necessitated the production of mixed micellar systems .[42]Therefore, the combination between two different types of pluronic polymers with great variation in HLB values was required to prepare a delivery system of pluronic micelle with reasonable thermodynamic stability and ideal kinetic. Therefore, different six micelles' formulations (F1–F6) composed of P188 and P123 were prepared by the previously mentioned technique with different ratios of P123:P188 (20:80 to 90:10) in total concentration 4% from the pluronics.

2.2. Determination of drug loading (%DL) and entrapment efficiency (%EE)

The results of % EE for the prepared TNPM (Table 3) revealed that TMZ as an example for the lipophilic drugs was successfully entrapped into the core of mixed pluronic micelles. There was an obvious improvement in %EE of TMZ was related to the increment in the concentration of pluronics P123 especially above 80% as result for the higher compatibility of TMZ with the core of the prepared pluronic micellar mixture. These results were related to the lipophilic nature of pluronic P123 and its characteristic structure that include long PPO block as well as short PEO moiety in combination with the lipophobic pluronic P188. This unique mixture provides a plausible stability, compatibility and entrapment for the loaded drug inside the core of the fabricated block. [43] Among, the prepared six TNPM formulations (F1-F6) with six different percent between P123 and P188, the formula F5 (80% P123 and 20%P188) achieved the highest %DL and %EE for both drugs compared to the others Table (3). Thus, F5 was selected for further formulations.

Table 3: Percentage of %DL and %EE of TNPM formulations (F1-F6)

Formula No	%DL ±SD, n=3		%EE ±SD, n=3	
	TMZ	NAC	TMZ	NAC
F1	5.8±0.038	14.8±0.4	28.34±2.3	73.56±6.1
F2	6.42±0.07	14±0.23	31.65±0.65	69.61±1.34
F3	**9.01**±0.043	12.74±0.51	45.3%±2.01	65.1±4.13
F4	9.63±0.2	12.42±0.47	51.54±1.56	63.77±2.54
F5	11.4±0.41	12.21±0.09	58.11±3.09	62.79±2.56
F6	11.26±0.52	11.17±0.25	57.54±1.98	56.89±3.73

2.3. *In vitro* characterizations of developed TNPM formulations using the selected percent (80% P123 and 20%P188) and different ratios of both drugs

2.3.1. Determination of drug loading and entrapment efficiency (%EE)

The results of % EE and DL% for the fabricated TNPM (Table 4) showed that L4 formula had the highest % EE and the lowest % EE for TMZ and NAC, respectively, also had the lowest DL% and the highest DL% for TMZ and NAC, respectively. Moreover, L5 showed results completely opposite to L4, as it had the lowest % EE and the highest % EE for TMZ and NAC, respectively, also had the highest DL% and the lowest DL% for TMZ and NAC, respectively. This is likely because the ratio of drugs (1:5 for TMZ and NAC, respectively) used in preparing L4 is opposite to the ratio of drugs (5:1 for TMZ and NAC, respectively) used in preparing L5. On the other hand, the results revealed that %EE of TMZ in L5 was less than %EE of TMZ in L8 despite the amount of TMZ used in the preparation being greater in L5 (16.6mg TMZ) than L8 (15mg TMZ), the %EE of TMZ in L5 might be significantly influenced by the presence of NAC and this may be due to the competition between the two drugs to occur in the core of the prepared micellar mixture. [44]

Table 4: Drug loading % and entrapment efficiency %of TNPM using the selected percent (80% P123 and 20% P188) and different ratios of both drugs.

Formula	EE%		DL%		Amount of drug in 1mg formula (mg)	
	TMZ	NAC	TMZ	NAC	TMZ	NAC
L1	86.34±2.1	45.21±4.5	10.91±0.5	11.76±0.72	0.1091±0.005	0.1176±0.0072
L2	88.99±4.6	40.61±2.7	10.3±0.7	12.58±0.51	0.103±0.007	0.1258±0.0051
L3	90.67±1.9	40.49±5.1	7.34±0.12	12.6±0.26	0.0734±0.0012	0.126±0.0026
L4	93.34±6.1	36.124±2.5	6.24±0.42	12.64±0.31	0.0624±0.0042	0.1264±0.0031
L5	32.13±1.	96.13±9.2	11.7±0.23	6.38±0.17	0.117±0.0023	0.0638±0.0017
L6	34.72±3.2	93.57±8.2	11.26±0.45	7.75±0.097	0.1126±0.0045	0.0775±0.00097
L7	0.00	94.32±6.8	0.00	9.7±0.43	0.00	0.097±0.0043
L8	41.3±5.2	0.00	10.43±0.12	0.00	0.1043±0.0012	0.00

2.3.2. *In vitro* Cytotoxicity

The *in vitro* cytotoxicity of eight formulations (L1 - L8), pure TMZ, pure NAC and pure formula against human glioblastoma multiforme A172 cell were evaluated by MTT assay after 48 h of incubation (Fig. 1). Viabilities of the tested cell line, treated with blank micelles up to 250 µg/mL were higher than 100%, indicating a high safety level of the pure formula and lack of intrinsic toxicities. These results are consistent with studies conducted on poloxamers from which micelles are prepared, which confirmed their safety.[45] This confirms the nanoform has an ideal composition, in contrast to other nanocarriers such as carbon nanotubes, quantum dots, liposomes, and PLGA nanoparticles, for which intrinsic toxicity has limited their use 65.

The cell viability declined in response to the treatment with other preparations in a concentration dependent manner. The nano formulation carrying one drug exerted a significantly more chemotherapeutic response compared to the respective free drugs. To kill 50% of A172 cells (IC_{50}), L8 and L7 required concentrations 16.7- and 32-fold lower than the IC_{50} of pure TMZ and NAC, respectively. This significant improvement in the anticancer activities might be attributed to the common phenomenon; the enhanced permeability and retention effect (EPR) which known for nanosystems treating cancer cells compared to respective free drugs. At the *in vitro* level, nano formulation tend to be more internalized than free drugs and this might mediate exerting a significantly more profound cytotoxic activity.[33]

It is worth mentioning that both L8 and L7 contained pluronic acid which is known to sensitize cancer cells even the multidrug resistant ones rendering them more responsive through several mechanisms such as inhibiting efflux pumps.[46]

In this study, nano formulations containing both TMZ and NAC combined in different ratios were prepared. Some of the combinations exhibited a significantly higher antitumoral effect compared to nanoforms containing a single drug, i.e., the nanoform of NAC (L7) and the nanoform containing TMZ (L8). That was the case of L1, L2, L3, L4, and L6. Specifically, the IC50 values of L1, L2, L3, L4, and L6 were lower than the IC50 of formula L7 (nanoform containing NAC only) by 7.2, 15, 23.5, 25.6, and 1.6-fold, respectively. Furthermore, the IC50 of L1, L2, L3, L4, and L6 were less than the IC50 of formula L8 (nanoform containing TMZ only) by 5.9, 12.4, 19.5, 21.3, and 1.3-fold, respectively. It was also noted that for some combinations, the anticancerous effect was significantly less than nanoforms of single drugs. That was the case of L5, where IC50 was higher than the IC50 of L8. Those findings highlight the importance of carefully combining drugs, and to fully understand the nature of this combination, calculating the combination index was followed.

To rigorously delineate the role of the micellar nanocarrier from inherent drug synergism, an unencapsulated free drug combination control (Free TMZ + Free NAC at a 1:5 w/w ratio, equivalent to L4) was included. While the free drug combination displayed moderate cytotoxicity (IC50 = 142.5±5.1ug/mL), the co-loaded micellar system L4 exhibited a nearly 7.8-fold lower IC50 = 18.3±0.089ugmL). Furthermore, L4 significantly outperformed single-drug micelles (L7 and L8) and free single drugs at equivalent concentrations, confirming that dual-drug micellar encapsulation facilitates synchronized cellular internalization and maximizes intracellular therapeutic synergy.

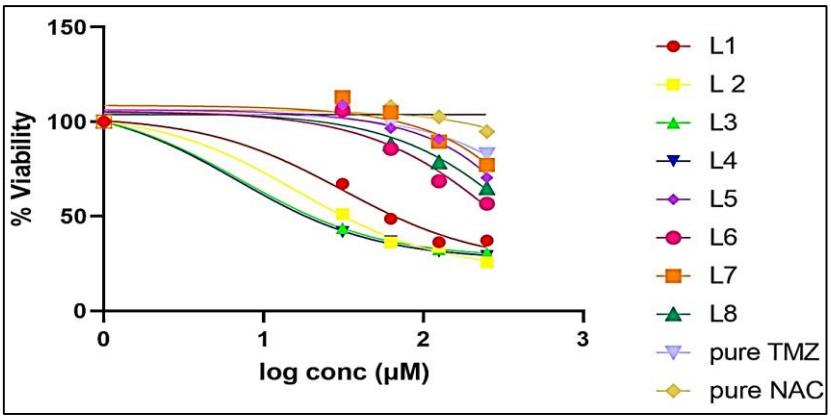

Fig. 1 The *in-vitro* cytotoxicity curve of eight formulations (L1 to L8) ,Pure TMZ and Pure NAC against human glioblastoma multiform A172 cell incubated for 48 h.

2.3.3. The combination index (CI)

The combination index value (CI) of the co-delivery carrier was further estimated to determine the synergism between TMZ and NA (Table 5). A clear synergistic effect was noted for the co-loaded TMZ and NAC in L1, L2, L3, and L4 because the calculated CI values were lower than 0.9, and antagonism was noted for the co-loaded TMZ and NAC in L5 and L6 because the calculated CI values were higher than 1.1.

In the case of L6, although the combination is an antagonistic one, the resultant IC50 was still less than individual IC50s. Because CI is calculated from viability data, the combination effect likely reflects the overall cellular response rather than binding to a specific receptor. NAC is an antioxidant and anti-inflammatory drug while TMZ is an alkylating chemotherapeutic generating oxidative stress. The exact role of NAC in cancer treatment is debatable where some studies conclude that NAC is a chemopreventive drug and when combined with chemotherapeutics, tends to lower their associated side effects.[47] At the same time, there are studies arguing for the ability of NAC to promote cancer development, progression and metastasis.[48] In our study, the L1-L4 mixing ratios produced a potent cytotoxic preparation, whereas the L5 ratio instead promoted cell proliferation. To fully understand those findings, further assays are needed to study the release kinetics of individual drugs, stability profile, and possibility of intra-molecular interaction with respect to different mixing ratios.

The TNPM formulations (L2, L3 and L4) exhibited the lowest drug IC50 values (65µg/ml, 19µg/ml and 18µg/ml), respectively. Because there was no significant difference between L3 and L4 in IC50 values, L2 and L4 formulations were selected for further evaluation studies.

It is crucial to interpret these cytotoxic and synergistic outcomes in light of the genetic profile of the A172 cell line. Since A172 cells are MGMT-methylated and MMR-proficient, they lack MGMT-mediated DNA repair, making them intrinsically responsive to TMZ alkylation. The observed enhancement in cell killing by L4 highlights the superiority of micellar co-delivery in sensitive glioblastoma cells; however, evaluating this dual-drug system in MGMT-overexpressing (unmethylated) and MMR-deficient chemoresistant models remains imperative for understanding its broader therapeutic scope.

Table 5: IC50 of eight formulations (L1 to L8) Pure TMZ and Pure NAC as well as combination index of L1, L2, L3, L4, L5, and L6 formulations

Formulations	IC_{50} of formula μg/ml	IC_{50} of TMZ μM	IC_{50} of NAC μM	CI	The effect
L1	65.79±2.1	36.93±1.3	47.41±2.4	0.376±0.003	synergism
L2	31.5±1.5	14.76±0.7	23.2857±1.4	0.1587±0.008	synergism
L3	19.94±1.09	7.538±0.3	15.151±1.1	0.0.092±0.001	synergism
L4	18.3±0.089	5.8815±0.09	14.173±0.95	0.0802±0.002	synergism
L5	408.4±16.8	246.11±12.4	159.66±7.2	2.4188±0.02	Strong antagonism
L6	293.73±9.6	185.37±6.9	139.144±4.8	1.824±0.014	antagonism
L7	469.43±17	-	279.028±12.6	-	-
L8	390.27±14	209.656±7.8	-	-	-
Pure TMZ	-	3505.2±145	-	-	-
Pure NAC	-	-	8962.37±362	-	-

2.4. Characterization of the selected TNPM formulations (L2 and L4)

2.4.1. Determination of particle size, polydispersity index (PDI) and zeta potential

Particle size and polydispersity index and zeta potential have a major effect on the biological behavior of nanoplatforms, exerting considerable influence on stability, bioavailability, *in vivo* distribution, and toxicity threshold.[49] The obtained results showed that the formulations L2 & L4 have average particle size of 309±156.6nm and 25.39±1.31nm, respectively. As found polydispersity index was 0.467 ± 0.002 and 0.259 ± 0.002, respectively. The difference in particle size between L2 and L4 may be due to their difference in drug loading: the DL% of TMZ in L2 (10.3) was greater than in L4 (6.24), because the hydrophobic drug settles inside the core of the PPO triblock. This step causes swelling of the PPO core and an increase in particle size and PDI value as a result of domain saturation.[50] The surface charge (ZP) of the formulations L2 and L4 was found to be -27.6 ± 8.47Mv and -24.5± 4.8Mv, respectively which was considered to be adequate to prevent particle aggregation and conserve the individual particles well–separated from each other without any agglomeration as a result of electric repulsion.[51]

The optimized formulation L4 displayed excellent batch-to-batch consistency with a high production yield of 91.4±2.8 % across three independent preparations. Upon 100-fold dilution in PBS (pH 7.4), L4 maintained its nanoscale dimensions (26.8±1.8 nm) and narrow PDI (0.264 ± 0.012), confirming strong thermodynamic and kinetic stability against premature dissociation in aqueous environments. This is directly supported by the exceptionally low critical micelle concentration (CMC = 0.00389wt%) of the P123:P188 (80:20) polymer blend

According to the previous characterization (TEM, particle size, zeta potential, DSC and FTIR analysis) for L2 and L4. The L4 formula showed better characteristics than L2. Thus, it was selected for further investigation. (Full TEM, DSC, and FT-IR data are provided in the Supplementary Data, Sections S2.3-S2.5.)

2.5. *In vitro* release studies

As explained in the following figure (Fig. 2), the pattern of *in vitro* release of TMZ and NAC from the selected formula L4 was assessed in comparison to the pure drugs (TMZ and NAC) in acetate buffer pH 4.5 which is

considered the most suitable medium for TMZ release.[52] The release medium was supported by 0.1% Tween 80 to cover the sink condition. Both, TMZ and NAC release from L4 formula was slower than pure drugs. The complete release of NAC was achieved within 4 h from the pure drug and 16 h from L4, respectively. On the contrary, the complete release pattern of TMZ from L4 was achieved after 30 h, however 50% of TMZ was liberated from the pure drug within the same period. Results revealed that the release pattern of TMZ and NAC from formula F4 showed a sustained release pattern which could be attributed to the structure of micelles that helped to retain the drugs inside the carriers, bringing a more persistent therapeutic effect than the pure drugs.[40] Furthermore, a comparison between the release profiles of TMZ and NAC from pure drugs and TMZ-NAC loaded L4 was carried out based on calculating the difference factor (f_1) and similarity factor (f_2). The calculation revealed that the difference factor (f_1) between pure TMZ and loaded-TMZ was 69.44 (more than 15) and between pure NAC and loaded-NAC was 29.77 (more than 15). While, the similarity factor (f_2) between pure TMZ and TMZ-L4 was 29.29 (less than 50) and pure NAC and NAC-L4 was 25.52 (less than 50). The obtained calculation elucidated that the two profiles are different and dissimilar and the entrapment of TMZ in PM resulted in a notable increase in its extent of drug release. Furthermore, it was clear that L4 showed higher release pattern characteristics for TMZ than pure TMZ. Also, the dissolution efficiency (%D.E.) calculation showed a lower release characteristic for NAC than pure NAC. The reduction in release efficiency for NAC from L4 may be because the release profile of NAC exhibited a biphasic pattern, with an initial fast release (85% after 12 h) followed by slower release up to 30 h. The slower release of NAC might be due to its powerful hydrophilic nature and strong interaction with the hydrophilic block (PEO) of polymeric micelle compared to TMZ.[33,53] The % dissolution efficiency for pure TMZ, pure NAC, TMZ-F and NAC-F was 38.36%, 95.32%, 68.4% and 78.06%, respectively. Thus, the fabrication of drug in pluronic micelle resulted in 1.783 folds improvement in the dissolution efficiency of TMZ (% D.E.).

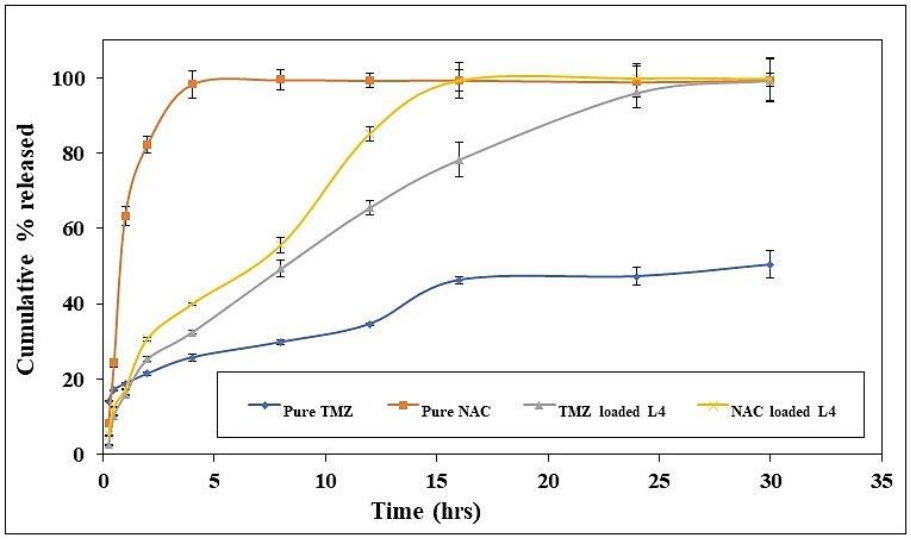

Fig. 2 *In-vitro* release profiles of TMZ and NAC from pure drugs and the selected TNPM (L4) in acetate buffer pH4.5 media at 37°C ± 0.5°C.

2.6. Release kinetics and mechanisms

The *in vitro* release results for pure drugs and L4 were fitted to Higuchi release kinetics model for TMZ and first order release kinetics models for NAC based on the highest correlation coefficient (R^2) values as indicated in table (S3). The *in vitro* release kinetics of TMZ and NAC from the selected formula L4 were further investigated

by applying the Korsmeyer –Peppas equations to the release data up to 60%. The obtained n value for TMZ-NAC loaded PM (L4) was 0.594 and 0.54 for TMZ and NAC, respectively, indicating a non-fickian model (anomalous transport) whereas the drug release from the formula is mainly controlled by a dual mechanism of polymer chain relaxation and diffusion.

2.7. Cell cycle analysis using Propidium Iodide

The Propidium Iodide-based cell cycle analysis was carried out to check the correct phase of cell cycle that affected by the formulation and pure drugs. Cells were treated with IC50 of pure TMZ, pure NAC, L4 and a control group was included (Fig. 3). Control, pure TMZ and pure NAC treated groups showed a similar cell cycle arrest pattern where the majority of the cells were arrested at G1 phase (between 70-85%) followed by S phase (13-21%) and a negligible % of the cells was arrested at G2 phase. This finding aligns with the previous studies of TMZ against A172 cells (27A). In case of L4, the cell cycle arrest pattern shifted so that 40% of the cells were arrested at G1 phase, 40% were at S phase, and 20% were at G2/M phase. This finding complements with the MTT results (Fig. 1) indicating the superiority of L4 over pure TMZ or NAC. Cells treated with L4 had their cell cycle arrested at multiple checkpoints, reflecting tighter suppression of proliferation. It is of great importance to block cell division of damaged DNA and prevent their progression into mitosis[54].

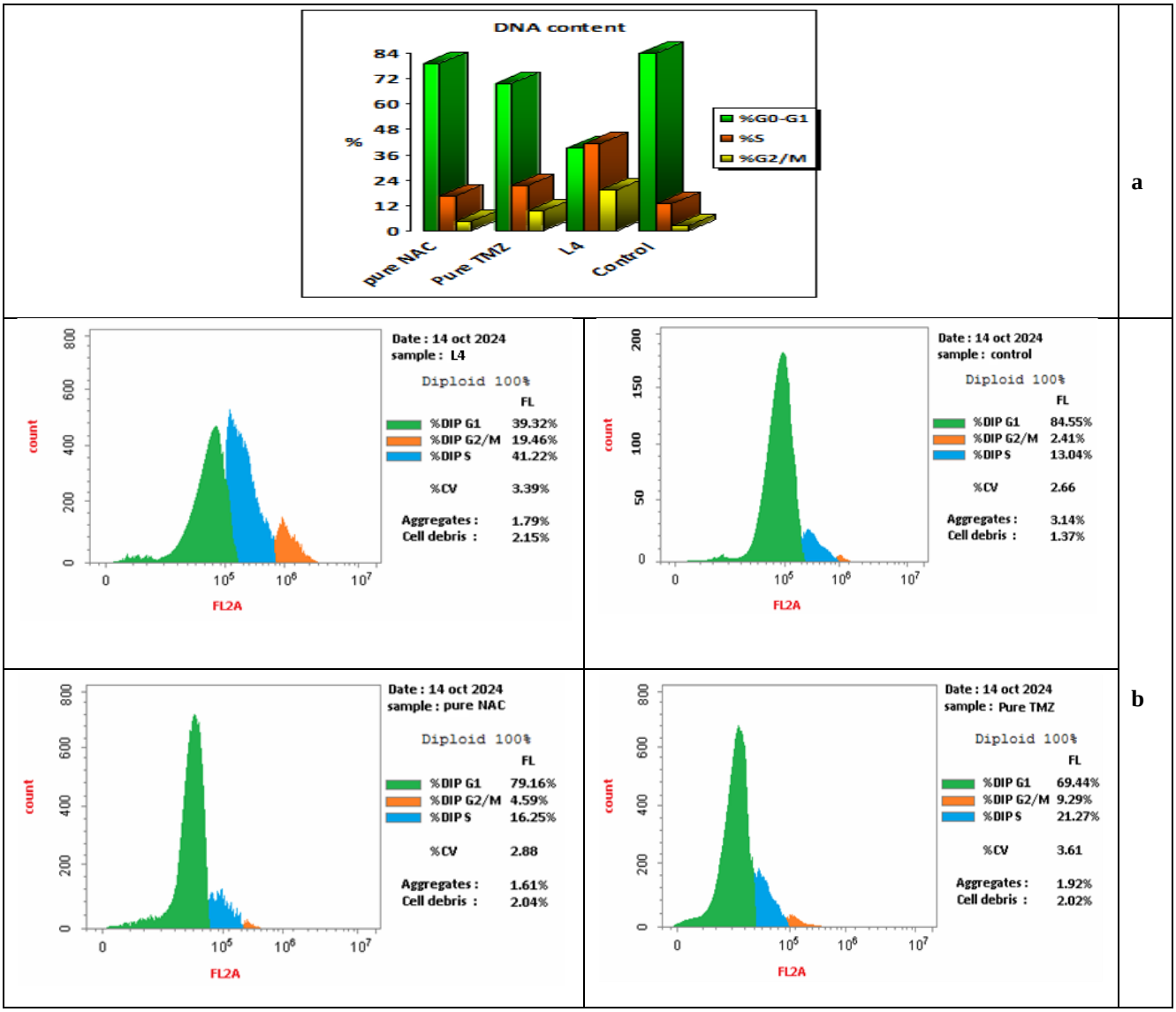

Fig. 3 The effect of L4, pure TMZ and pure NAC on human glioblastoma multiform A172 cell, (a) histogram represents the specific cell cycle phase, (b) represents the quantitative cells counting at each phase as compared to control.

2.8. Human glioblastoma cell death mode in response to treatment

Annexin-V vs Propidium Iodide (PI) based assay was carried out to study and determine the accurate mode of cell death raised by the treatment with the selected formulations. The main principle of the test depends on the interaction and binding of Annexin V with phosphatidyl serine, which is a major protein that drains from the cytosol to cell surface during the apoptosis process. Once the membrane becomes permeabilized, PI invades the cell and intercalates the DNA signifying the necrosis. This assay was applied for human glioblastoma multiforme A172 cells treated with the determined IC50 concentrations of Pure TMZ, Pure NAC and L4 compared to a control group (Fig.4). The control group showed the highest percentage (approximately 96.72%) of viable cells. Upon treatment, this % declined to 89, 80, and 71% for cells treated with Pure NAC, Pure TMZ and L4, respectively. It should be noted that those percentages differ from the ones obtained by MTT assay (Fig. 4) since the mode of cell viability detection is different in both assays. An accompanying increase in the apoptotic cell population was observed in all treated groups which suggests that they induce apoptosis. This finding agrees with previous studies confirming that TMZ induces apoptotic cell death mode.[55] The apoptotic cell population of L4 treated was 23% which is double and three times the apoptotic population of cells treated with Pure TMZ and Pure NAC, respectively. This finding further emphasizes the outperformance of L4.

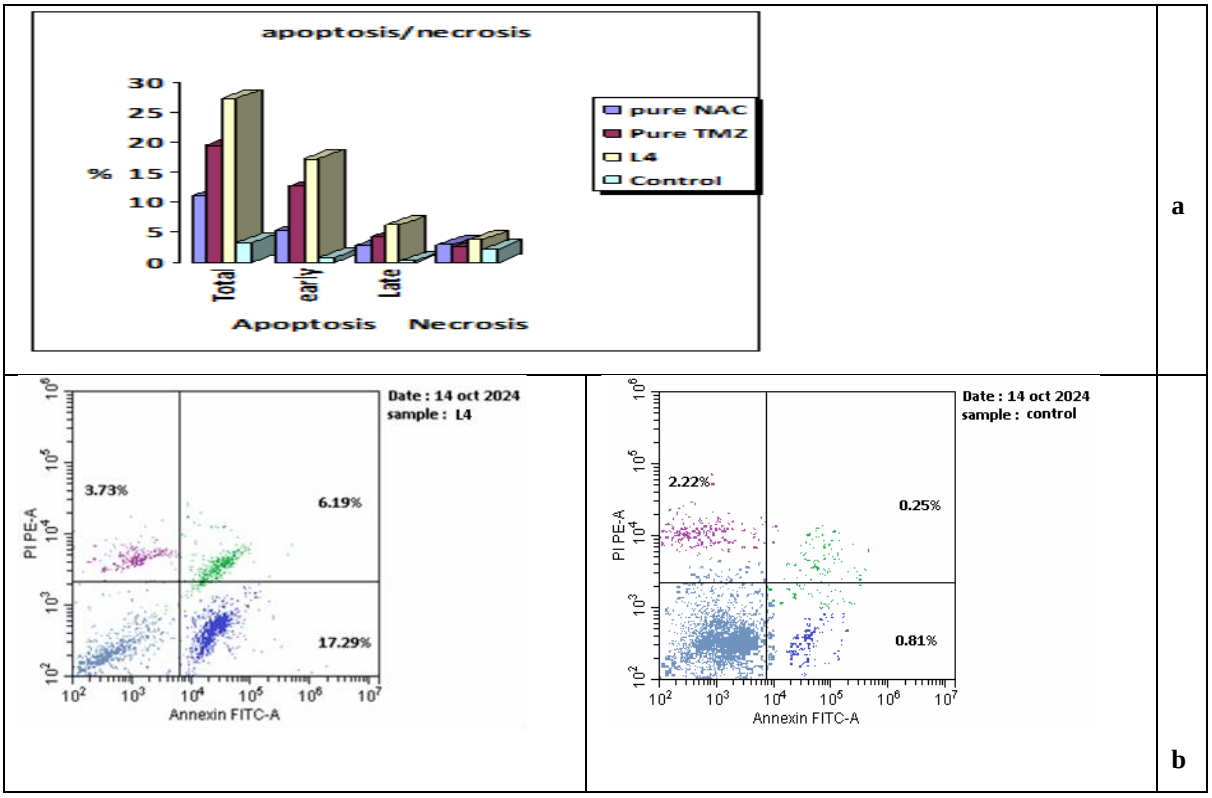

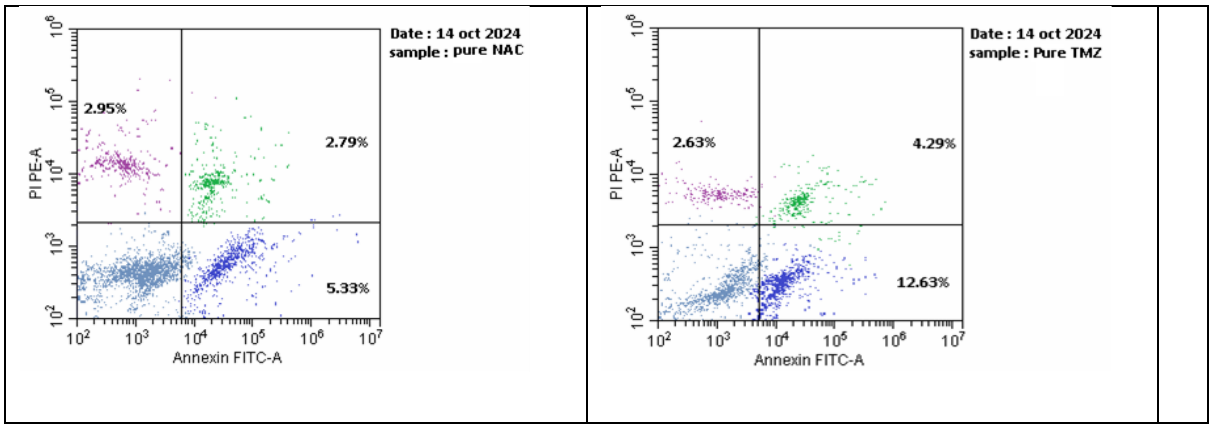

Fig. 4 (a) Histogram representing the effect of L4, pure TMZ and pure NAC treatment on cell pattern death (apoptosis and necrosis) carried out on Human glioblastoma multiform A172 cell. Apoptosis was measured using Annexin V and necrosis by PI stain. (b) represents the quantitative analysis suggesting the percentage of each type of cell in each quadrant

Representative photo-images of the control and treated cells showed pronounced morphological changes and loss of intercellular connections in response to treatment. Morphological features characterizing apoptotic cell death mode include apoptotic bodies, shrinkage of the cells and loss of integrity [56]. The futuristic work investigating Caspase-dependence will help draw a detailed image about the mechanism of action of the highly antitumoral formulation L4 (Fig.5).

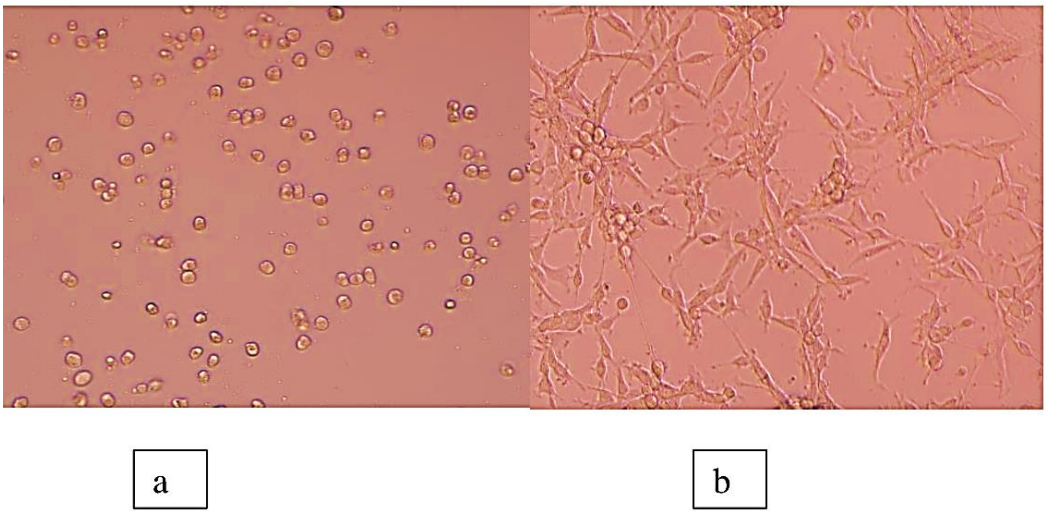

Fig. 5 a) Human glioblastoma multiform A172 cell Treated by L4, b) Control Human glioblastoma multiform A172 cell. Magnification power was 20x and images were captured with Invitrogen converted microscope using light field settings

2.9. Cellular uptake

HPLC based calibration curves for TMZ (0.5-20 µg/mL) and NAC (1-100 µg/mL) were established. For TMZ, the retention time (RT) was 4.0659 min and linearity (R2) was 0.9995. For NAC, RT was approximately 3.4336 min, with a linearity (R2) of 0.9986. The cellular uptake efficiency of TMZ and NAC from the selected TNPM (L4) and pure TMZ and pure NAC after 12 and 24 h was determined (Table 6). The cellular uptake of TMZ and NAC by A172 cells markedly elevated, as the incubation time increased from 12 h to 24 h. Also, the cell uptake of TMZ and NAC significantly increased in TMZ-NAC-loaded micelles (L4) compared to pure TMZ and pure NAC. Results showed that the cumulative intracellular uptake efficiency of pure TMZ and pure NAC after 24 h was 2.94% and 5.92%, respectively. On the other hand, cellular uptake efficiency of TMZ and NAC from the selected TMZ-NAC-loaded pluronic micelles (L4) at the same time interval was 89.72% and 89%, respectively. The improvement in the cellular uptake might be attributed to the nano-size fabricated vesicle.[57] The

smaller particle size of the fabricated L4 formula provided distinctive chances to interact with A172 cells and to be internalized in comparison to pure TMZ and pure NAC.

Furthermore, micelles carried positive charge which enhances cellular uptake with negatively charged cell membrane.[58] Finally, it was clear that the cellular uptake efficiency of TMZ and NAC from the selected TMZ-NAC-loaded micelles (L4) after 12 hrs was 30.48 and 15 folds higher than that of pure TMZ and pure NAC, respectively.

Table 6: Cellular uptake efficiency % of pure TMZ, pure NAC, TNPM (L4) after 12 hrs and 24 hrs.

Time (hrs)	% Cellular uptake efficiency			
	TMZ in L4	**NAC in L4**	**Pure TMZ**	**Pure NAC**
12	57.31255937	75.82899726	2.328474395	3.480723457
24	89.72677398	89.00805392	2.943304935	5.927075206

Conclusion

The current study successfully develo*p*ed TNPM (L4) to carry combination therapy, improve dissolution rate of TMZ and eventually enhance the cytotoxicity of TMZ by the synergism of TMZ and NAC against human glioblastoma multiforme A172 cells. Fabrication of formulations F1 to F6 facilitated the selection of 80:20 (F5) as the most adequate ratio of P123 to P188 that could be loaded with both drugs. The formula (L4) that was fabricated from 4%w/w polymeric micelle and loaded with TMZ and NAC at a ratio of 1:2 (w/w, TMZ:NAC). This formula exhibited the highest drug entrapment and showed promising *in vitro* release and cellular uptake with 1.783-fold and 30.48-fold increase in dissolution efficiency % and cellular uptake efficiency % of TMZ, respectively. Cell cycle and Cell apoptosis studies confirmed the potential of L4 for cytotoxicity against human glioblastoma multiforme A172 cells. Additionally, further studies employing MGMT-unmethylated/resistant glioblastoma models (such as T98G) and MMR-deficient lines, alongside in-vivo absorption and biodistribution studies, will be essential to fully establish the potential of TNPM (L4) in overcoming MGMT-mediated resistance. Thus, the formula L4 could be used to treat brain tumors if encapsulated in suitable dosage form. However, further *in vivo* absorption and biodistribution studies in animals and humans and clinical trials in patients should be achieved to support the obtained results and transfer the finding to the industry.

Manuscript limitation and future work

For the calculation of confidence intervals, we claim that the ± values reported in Table 5 reflect the standard deviation of IC50 determinations across triplicate wells (n = 3), not a formal confidence interval around the CI value itself. We agree that a rigorous synergy determination should ideally report CI with a propagated confidence interval (e.g., via the median-effect analysis software with variance estimation, such as CompuSyn).

The study exhibited the efficacy of the formula against single cell line of glioblastoma (A172) due to the limitation for the availability of other cell lines. However, we conducted a study of the best formula L4 against the viability of the skin fibroblast cell line as it is the only accessible normal human cell line. Results indicated that the viability was above 90% up to a concentration of (1 mg/mL). For higher concentrations, the viability dropped. Yet up to the highest tested concentration, the viability was above 50%. This finding reflects the safety nature of the formulation. Moreover, We have explicitly revised the Discussion and Conclusion sections to state that testing this optimized dual-loaded micellar system (L4) on MGMT-unmethylated/TMZ-resistant glioblastoma lines (such

as T98G), additional GBM cell lines (such as U87MG), and normal primary human astrocytes represents the core objective of our upcoming follow-up study prior to *in vivo* evaluations.

Acknowledgments

The authors would like to express their sincere gratitude to **Retaj Elshourbagi**, a fifth-year Clinical PharmD student at Galala University, for her careful proofreading of the manuscript and valuable suggestions that improved the clarity and readability of the English language. The authors also gratefully acknowledge **Gamal Sheridan**, a third-year Graphics Information Technology student at Arizona State University and Galala University, for his meticulous review of the manuscript and assistance in refining the English language and overall readability.

The authors disclose the use of ChatGPT (OpenAI, GPT-5.5) and Claude AI (Anthropic) during the preparation of this manuscript. These tools were used solely to clarify some reviewers' comments, improving the wording of selected responses to reviewers, refining the language of selected sentences in the manuscript and checking the consistency and formatting of references. Following the use of these AI tools, all generated or edited text was carefully reviewed, verified, and manually revised by the authors. The authors remain fully responsible for the accuracy, originality, and integrity of all content presented in this manuscript.

Funding

"The authors declare that no funds, grants, or other support were received during the preparation of this manuscript."

Ethics approval

The manuscript does not include animal study.

Competing interest

"The authors have no relevant financial or non-financial interests to disclose."

Availability of data and materials

The datasets generated during and/or analyzed during the current study are available from the corresponding author on reasonable request.

Authors' contributions

Mohammed S. Teiama: conceptualization, design the frame of the work, share in data analysis, writing, revising work for intellectual contents and contribute to data interpretation to accomplish final approval for the published version. **Wedad Sakran:** Conceptualization, design the work, revising the work critically for important intellectual contents, analysis and interpretation for the data and attain final approval for the published version. **Fares Ibrahim:** methodology, investigation, experimental work, share in data analysis. **Sara A. Abdel Gaber:** design the frame work for cell culture and cancer cell line experiments, perform part in methodology, writing, revising work for intellectual contents and contribute to data interpretation to accomplish final approval for the published version. **Raghda abd el moneum:** conceptualization, share in work design, share in data analysis, writing, reviewing and editing the work, contribute to data examination and interpretation to get the final approval for the published version.

Reference

1. Singh SK, Mohammed A, Alghamdi OA, Husain SM. New approaches for targeting drug resistance through drug combination. In: *Combination Therapy Against Multidrug Resistance*. Elsevier; 2020. P. 221-46. https://doi.org/10.1016/B978-0-11-823560-6.00010-3
2. Mohammed A, Hamdan A, Homoud A. Histopathological profile of brain tumors: a 12-year retrospective study from Madinah, Saudi Arabia. *Asian J Neurosurg* 2019;14(4):1106-11. https://doi.org/10.4103/ajns.AJNS_230_19

3. De Vleeschouwer S, Bergers G. Glioblastoma: to target the tumor cell or the microenvironment? *Exon Publ* Published online 2017:315-40. https://doi.org/10.15586/codon.glioblastoma.2017.ch16
4. Arstall MA, Yang J, Stafford I, Betts WH, Horowitz JD. N-acetylcysteine in combination with nitroglycerin and streptokinase for the treatment of evolving acute myocardial infarction: safety and biochemical effects. *Circulation* 1995;92(10):2855-62. https://doi.org/10.1161/01.cir.92.10.2855
5. Urbańska K, Sokołowska J, Szmidt M, Sysa P. Glioblastoma multiforme–an overview. *Contemp Oncol Onkol* 2014;18(5):307-12. https://doi.org/10.5114/wo.2014.40558
6. Ramalho MJ, Andrade S, Coelho MÁN, Loureiro JA, Pereira MC. Biophysical interaction of temozolomide and its active metabolite with biomembrane models: The relevance of drug-membrane interaction for Glioblastoma Multiforme therapy. *Eur J Pharm Biopharm* 2019;136:156-63. https://doi.org/10.1016/j.ejpb.2019.01.018
7. Oliver L, Lalier L, Salaud C, Heymann D, Cartron PF, Vallette FM. Drug resistance in glioblastoma: are persisters the key to therapy? *Cancer Drug Resist* 2020;3(3):287. https://doi.org/10.20517/cdr.2020.13
8. Büsker S, Jäger W, Poschner S, Mayr L, Al Jalali V, Gojo J, et al. Pharmacokinetics of metronomic temozolomide in cerebrospinal fluid of children with malignant central nervous system tumors. *Cancer Chemother Pharmacol* 2022;89(5):617-27. https://doi.org/10.1007/s00280-022-04423-8
9. Lingertat-Walsh K, Weilnau J, Cober MP, Ostrenga A, Poon B, Sales P, et al. Stability of extemporaneously compounded temozolomide 10 mg/mL suspensions in Oral Mix SF® in glass and plastic bottles and plastic syringes. *J Oncol Pharm Pract* 2021;27(1):78-87. https://doi.org/10.1177/1078155220918151
10. Wesolowski JR, Rajdev P, Mukherji SK. Temozolomide (temodar). *Am J Neuroradiol* 2010;31(8):1383-4. https://doi.org/10.3174/ajnr.A2170
11. Muggeri A, Vago M, Pérez S, Rubio M, González C, Magarinos C, et al. A randomized, open-label, two-way crossover, single-dose bioequivalence study of temozolomide 200 mg/m2 (Dralitem® vs. Temodal® capsules) in patients with primary tumors of the central nervous system under fasting conditions. *Drugs R D* 2017;17(3):427-34. https://doi.org/10.1007/s40268-017-0198-4
12. Newton HB. Handbook of Brain Tumor Chemotherapy, Molecular Therapeutics, and Immunotherapy. Academic Press; 2018. https://doi.org/10.1016/C2016-0-03719-7
13. Khan A, Aqil M, Imam SS, Ahad A, Sultana Y, Ali A, et al. Temozolomide loaded nano lipid based chitosan hydrogel for nose to brain delivery: Characterization, nasal absorption, histopathology and cell line study. *Int J Biol Macromol* 2018;116:1260-7. https://doi.org/10.1016/j.ijbiomac.2018.05.082
14. Guerini M, Condrò G, Friuli V, Maggi L, Perugini P. N-Acetylcysteine (NAC) and its role in clinical practice management of cystic fibrosis (CF): a review. *Pharmaceuticals* 2022;15(2):217. https://doi.org/10.3390/ph15020217
15. Ooi SL, Green R, Pak SC. N-acetylcysteine for the treatment of psychiatric disorders: A review of current evidence. *Biomed Res Int* 2018;2018(1):2469486. https://doi.org/10.1155/2018/2469486
16. van Zandwijk N. N-acetylcysteine for lung cancer prevention. *Chest* 1995;107(5):1437-41. https://doi.org/10.1378/chest.107.5.1437
17. Garrido M, Tereshchenko Y, Zhevtsova Z, Taschenberger G, Bähr M, Kügler S. Glutathione depletion and overproduction both initiate degeneration of nigral dopaminergic neurons. *Acta Neuropathol* 2011;121(4):475-85. https://doi.org/10.1007/s00401-010-0792-2
18. Al Bostami RD, Abuwatfa WH, Husseini GA. Recent advances in nanoparticle-based co-delivery systems

for cancer therapy. *Nanomaterials* 2022;12(15):2672. https://doi.org/10.3390/nano12152672

19. Sun J, Liu Y, Chen Y, Zhao W, Zhai Q, Rathod S, et al. Doxorubicin delivered by a redox-responsive dasatinib-containing polymeric prodrug carrier for combination therapy. *J Control Release* 2017;258:43-55. https://doi.org/10.1016/j.jconrel.2017.05.006
20. Kedar U, Phutane P, Shidhaye S, Kadam V. Advances in polymeric micelles for drug delivery and tumor targeting. *Nanomedicine Nanotechnology, Biol Med* 2010;6(6):714-29. https://doi.org/10.1016/j.nano.2010.05.005
21. Torchilin VP. Structure and design of polymeric surfactant-based drug delivery systems. *J Control release* 2001;73(2-3):137-72. https://doi.org/10.1016/S0168-3659(01)00299-1
22. Kabanov A V, Batrakova E V, Alakhov VY. Pluronic® block copolymers for overcoming drug resistance in cancer. *Adv Drug Deliv Rev* 2002;54(5):759-79. https://doi.org/10.1016/S0169-409X(02)00047-9
23. Ten Tije AJ, Verweij J, Loos WJ, Sparreboom A. Pharmacological effects of formulation vehicles: implications for cancer chemotherapy. *Clin Pharmacokinet* 2003;42(7):665-85. https://doi.org/10.2165/00003088-200342070-00005
24. Aliabadi HM, Lavasanifar A. Polymeric micelles for drug delivery. *Expert Opin Drug Deliv* 2006;3(1):139-62. https://doi.org/10.1517/17425247.3.1.139
25. Fan Z, Chen C, Pang X, Yu Z, Qi Y, Chen X, et al. Adding vitamin E-TPGS to the formulation of Genexol-PM: specially mixed micelles improve drug-loading ability and cytotoxicity against multidrug-resistant tumors significantly. *PLoS One* 2015;10(4):e0120129. https://doi.org/10.1371/journal.pone.0120129
26. Mursaleen L, Noble B, Chan SHY, Somavarapu S, Zariwala MG. N-Acetylcysteine nanocarriers protect against oxidative stress in a cellular model of Parkinson's disease. *Antioxidants* 2020;9(7):600. https://doi.org/10.3390/antiox9070600
27. Nasr M, Ghorab MK, Abdelazem A. In vitro and in vivo evaluation of cubosomes containing 5-fluorouracil for liver targeting. *Acta Pharm Sin B* 2015;5(1):79-88. https://doi.org/10.1016/j.apsb.2014.12.001
28. Ferreira LF, Campbell KS, Reid MB. N-acetylcysteine in handgrip exercise: plasma thiols and adverse reactions. *Int J Sport Nutr Exerc Metab* 2011;21(2):146-54. https://doi.org/10.1123/ijsnem.21.2.146
29. Zainuddin R, Zaheer Z, Sangshetti JN, Momin M. Enhancement of oral bioavailability of anti-HIV drug rilpivirine HCl through nanosponge formulation. *Drug Dev Ind Pharm* 2017;43(12):2076-84. https://doi.org/10.1080/03639045.2017.1368097
30. Kammerer R, Buchner A, Palluch P, Pongratz T, Oboukhovskij K, Beyer W, et al. Induction of immune mediators in glioma and prostate cancer cells by non-lethal photodynamic therapy. *PLoS One* 2011;6(6):e21834. https://doi.org/10.1371/journal.pone.0021834
31. Serag E, Gaber SAA, Abdel-Shafi AA, El-Khouly ME. Perylene tetracarboxylic acid-folate conjugated carbon quantum dots for targeted photodynamic therapy of prostate Cancer. *Bioorg Chem* Published online 2025:108631. https://doi.org/10.1016/j.bioorg.2024.108631
32. Chou TC. Drug combination studies and their synergy quantification using the Chou-Talalay method. *Cancer Res* 2010;70(2):440-6. https://doi.org/10.1158/0008-5472.CAN-09-1947
33. Almoshari Y, Iqbal H, Razzaq A, Ali Ahmad K, Khan MK, Saeed Alqahtani S, et al. Development of

nanocubosomes co-loaded with dual anticancer agents curcumin and temozolomide for effective colon cancer therapy. *Drug Deliv* 2022;29(1):2633-43. https://doi.org/10.1080/10717544.2022.2100513

34. Shaker DS, Shaker MA, Hanafy MS. Cellular uptake, cytotoxicity and in-vivo evaluation of Tamoxifen citrate loaded niosomes. *Int J Pharm* 2015;493(1-2):285-94. https://doi.org/10.1016/j.ijpharm.2015.07.041
35. Amidon GL, Lennernäs H, Shah VP, Crison JR. A theoretical basis for a biopharmaceutic drug classification: the correlation of in vitro drug product dissolution and in vivo bioavailability. *Pharm Res* 1995;12(3):413-20. https://doi.org/10.1023/A:1016212804288
36. Khan KA. The concept of dissolution efficiency. *J Pharm Pharmacol* 1975;27(1):48-9. https://doi.org/10.1111/j.2042-2156.1975.tb00996.x
37. Sharma R, Walker RB, Pathak K. Evaluation of the kinetics and mechanism of drug release from econazole nitrate nanosponge loaded carbapol hydrogel. Published online 2011.
38. Korsmeyer RW, Gurny R, Doelker E, Buri P, Peppas NA. Mechanisms of solute release from porous hydrophilic polymers. *Int J Pharm* 1983;15(1):25-35. https://doi.org/10.1016/0378-5173(83)90064-9
39. Gaber SAA, Nasr M, Hamzawy MA. Pterostilbene lipid nanocapsules as a promising system for treatment of hepatocellular carcinoma: formulation, characterization, and cellular/in vivo appraisal. *J Drug Deliv Sci Technol* 2024;92:105310. https://doi.org/10.1016/j.jddst.2024.105310
40. Nasr M, Hashem F, Abdelmoniem R, Tantawy N, Teiama M. In vitro cytotoxicity and cellular uptake of tamoxifen citrate-loaded polymeric micelles. *Aaps Pharmscitech* 2020;21(8):306. https://doi.org/10.1208/s12249-020-01851-x
41. Michels LR, Fachel FNS, Azambuja JH, Gelsleichter NE, Braganhol E, Teixeira HF. HPLC–UV method for temozolomide determination in complex biological matrices: Application for in vitro, ex vivo and in vivo studies. *Biomed Chromatogr* 2019;33(10):e4615. https://doi.org/10.1002/bmc.4615
42. Attia ABE, Ong ZY, Hedrick JL, Lee PP, Ee PLR, Hammond PT, et al. Mixed micelles self-assembled from block copolymers for drug delivery. *Curr Opin Colloid Interface Sci* 2011;16(3):182-94. https://doi.org/10.1016/j.cocis.2011.01.006
43. Allen C, Maysinger D, Eisenberg A. Nano-engineering block copolymer aggregates for drug delivery. *Colloids Surfaces B Biointerfaces* 1999;16(1-4):3-27. https://doi.org/10.1016/S0927-7765(99)00058-2
44. Meteoglu I, Erdemir A. Genistein and temozolomide-loaded polymeric nanoparticles: a synergistic approach for improved anti-tumor efficacy against glioblastoma. *Process Biochem* 2021;110:9-18. https://doi.org/10.1016/j.procbio.2021.07.018
45. Singh-Joy SD, McLain VC. Safety assessment of poloxamers 101, 105, 108, 122, 123, 124, 181, 182, 183, 184, 185, 188, 212, 215, 217, 231, 234, 235, 237, 238, 282, 284, 288, 331, 333, 334, 335, 338, 401, 402, 403, and 407, poloxamer 105 benzoate, and poloxamer 182 dibenzoate as use. *Int J Toxicol* 2008;27:93-128. https://doi.org/10.1080/10915810802244595
46. Mehanny M, Hathout RM, Geneidi AS, Mansour S. Exploring the use of nanocarrier systems to deliver the magical molecule; curcumin and its derivatives. *J Control release* 2016;225:1-30. https://doi.org/10.1016/j.jconrel.2016.01.018
47. Kalyanaraman B. NAC, NAC, Knockin'on Heaven's door: interpreting the mechanism of action of N-acetylcysteine in tumor and immune cells. *Redox Biol* 2022;57:102497. https://doi.org/10.1016/j.redox.2022.102497
48. Zhang VX, Sze KMF, Chan LK, Ho DWH, Tsui YM, Chiu YT, et al. Antioxidant supplements promote

tumor formation and growth and confer drug resistance in hepatocellular carcinoma by reducing intracellular ROS and induction of TMBIM1. *Cell Biosci* 2021;11(1):217. https://doi.org/10.1186/s13578-021-00728-6

49. Alexis F, Pridgen E, Molnar LK, Farokhzad OC. Factors affecting the clearance and biodistribution of polymeric nanoparticles. *Mol Pharm* 2008;5(4):505-15. https://doi.org/10.1021/mp800051m
50. Pellosi DS, Paula LB, de Melo MT, Tedesco AC. Targeted and synergic glioblastoma treatment: multifunctional nanoparticles delivering verteporfin as adjuvant therapy for temozolomide chemotherapy. *Mol Pharm* 2019;16(3):1009-24. https://doi.org/10.1021/acs.molpharmaceut.8b01020
51. Zidan MF, Ibrahim HM, Afouna MI, Ibrahim EA. In vitro and in vivo evaluation of cyclodextrin-based nanosponges for enhancing oral bioavailability of atorvastatin calcium. *Drug Dev Ind Pharm* 2018;44(8):1243-53. https://doi.org/10.1080/03639045.2018.1442841
52. Waghule T, Saha RN, Singhvi G. UV spectroscopic method for estimation of temozolomide: Application in stability studies in simulated plasma pH, degradation rate kinetics, formulation design, and selection of dissolution media. *Spectrochim Acta Part A Mol Biomol Spectrosc* 2021;258:119848. https://doi.org/10.1016/j.saa.2021.119848
53. Ghezzi M, Pescina S, Padula C, Santi P, Del Favero E, Cantù L, et al. Polymeric micelles in drug delivery: An insight of the techniques for their characterization and assessment in biorelevant conditions. *J Control Release* 2021;332:312-36. https://doi.org/10.1016/j.jconrel.2021.02.031
54. Haschka M, Karbon G, Fava LL, Villunger A. Perturbing mitosis for anti-cancer therapy: is cell death the only answer? *EMBO Rep* 2018;19(3):e45440. https://doi.org/10.15252/embr.201745440
55. Xue Y, Lu Y, Sun G, Fang F, Ji Y, Tang H, et al. CN-3 increases TMZ sensitivity and induces ROS-dependent apoptosis and autophagy in TMZ-resistance glioblastoma. *J Biochem Mol Toxicol* 2022;36(3):e22973. https://doi.org/10.1002/jbt.22973
56. Chen Y, Li X, Yang M, Liu SB. Research progress on morphology and mechanism of programmed cell death. *Cell Death Dis* 2024;15(5):327. https://doi.org/10.1038/s41389-024-05336-6
57. Wang N, Wang Z, Nie S, Song L, He T, Yang S, et al. Biodegradable polymeric micelles coencapsulating paclitaxel and honokiol: a strategy for breast cancer therapy in vitro and in vivo. *Int J Nanomedicine* Published online 2017:1499-514. https://doi.org/10.2147/IJN.S128608
58. Fröhlich E. The role of surface charge in cellular uptake and cytotoxicity of medical nanoparticles. *Int J Nanomedicine* Published online 2012:5577-91. https://doi.org/10.2147/IJN.S36111